RESEARCH PAPER

Magnetic Characteristics of Nanocrystalline $Co_{78}Zr_{17}B_2Si_1W_2$ Alloy Formed by Melt Spinning and Subsequent Annealing

Mohamad Molaahmadi*, Ali Ghasemi, Majid Tavoosi, Gholam Reza Gordani

* m.molaahmadi1@gmail.com

Department of Materials Engineering, Malek- Ashtar University of Technology, Shahin-Shahr, Isfahan, Iran

Abstract: The investigation of the structural and magnetic properties of nanocrystalline $Co_{78}Zr_{17}B_2Si_1W_2$ alloy during melt spinning and annealing processes were the main goals of this study. In this regard, samples were prepared using vacuum induction melting, melt spinning and subsequent annealing. The specimens were evaluated using X-ray diffraction (XRD), field emission scanning electron microscope (FESEM), differential scanning calorimetry (DSC) and vibrating sample magnetometer (VSM). Based upon the results obtained, nano-crystalline Co_5Zr single phase with hard magnetic properties (Ms= 29.5 emu/g and Hc= 2.7 kOe) was formed during melt spinning process (at wheel speed of 40 m.s⁻¹). The coercivity value of rapidly solidified sample increased to about 3.2 kOe during annealing process up to 400°C. However, higher annealing temperature led to the transformation of non-equilibrium magnetic Co_5Zr phase to a more stable Zr_2Co_{11} phase, which has negative effects on final magnetic properties.

Keywords: Co-Zr alloy, Nanocrystalline, Melt-spinning, Magnetic properties.

1. INTRODUCTION

Developing novel rare-earth-free permanent magnets is a new challenge in the field of magnetic materials [1]. Co-Zr alloys are suitable candidates for the development of permanent magnets without rare earth elements due to their relatively strong uniaxial anisotropy (11 Merg/cm³) and high Curie temperature (773 K) [2]. Nevertheless, the saturation magnetization and maximum generated energy prepared in this system are lower than that of rate-earth based magnets [3].

Based on Lucis [4] report, non-equilibrium ZrCo₅ compound with high magneto-crystalline anisotropy is the most important magnetic phase in the Co-Zr system. Despite the soft magnetic properties of common cobalt-based alloys, the Co₅Zr intermetallic compounds are well-known hard magnetic phase that can be a good alternative to rare earth-based magnets [5]. The Co₅Zr phase is formed in a pritectic transformation during casting. However, in normal solidification process, phase separation occurs and a large portion of the un-reacted δ-phase (pro-pritectic) and un-wanted Co, Co₁₁Zr₂ and Zr₆Co₂₃ phases, with low magneto-crystalline anisotropies, remains in the microstructure [6]. Therefore, non-equilibrium process techniques such as melt-spinning have been introduced to achieve permanent magnets in the Co-Zr alloy system [7].

Over the past few decades, extensive studies have been conducted on the effect of adding various elements on magnetic properties of Co-Zr alloy system. For example, Lucis et al. [4] confirmed the positive effects of Mo, Si and B elements on hard magnetic properties of Co-Zr system. Zhang et al. [8] also showed that the addition of Mo to Co₇₈Zr₁₆Si₃B₃ significantly reduces the potential for the formation of a cobalt-rich soft magnetic phase, thereby increasing the coercivity. The effect of tungsten on the magnetic properties of Co-Zr alloys was also investigated by Shifeng et al [9], whereby the maximum coercivity in the Co₇₇Zr₁₈W₅ alloy was reported to be about 4.3 kOe.

However, the present work focuses on the investigation about the structural and magnetic characteristics of nanocrystalline Co₇₈Zr₁₇B₂Si₁W₂ alloy during melt spinning process. Study on the thermal stability of formed phases during the melt-spinning process is another issue which is evaluated in this research.

2. EXPERIMENTAL PROCEDURES

In this research, high purity (above 99%) Co, Zr, Si, B and W ingots were used as row materials. Arc melting process under argon atmosphere was used to prepare Co₇₈Zr₁₇B₂Si₁W₂ primary ingot. To ensure homogeneity, the melting was carried out 4 times. The melt-spun ribbons were produced

1

by injecting the melt onto a rotating copper wheel of 240 mm diameter with substrate velocities of 40 m.s^{-1} in argon atmosphere. The pressure of spinner chamber before melt injection was about 5×10^{-3} Pa which increased to 10^5 Pa during melt spinning process. Annealing procedure had been done at temperatures range of 400 to 700°C under argon atmosphere.

An XRD using a diffractometer with Cu K$_\alpha$ radiation (λ= 0.15406 nm; 40 kV; Philips PW3710) was used to follow the structural variation of the specimens (step size: 0.05°; time per step: 0.5 s). The crystallite sizes ZrCo$_5$ phase estimated form XRD pattern using Scherrer method [12]. Structural characterizations of samples were carried out by field emission scanning electron microscopy (VEGA-TESCAN-XMU) at an accelerating voltage of 20 kV. Differential scanning calerimerty was also conducted to study the thermal stability of produced amorphous alloy using the L81/1750 DTA differential thermal analyzer. The samples were placed in Al$_2$O$_3$ pans and heated in dynamic argon atmosphere up to 900°C at a heating rate of 20°C/min. Magnetic properties of produced samples were measured using a vibrating scanning manometer under an applied field up to 10 kOe.

3. RESULTS AND DISCUSSION

The XRD patterns of Co$_{78}$Zr$_{17}$B$_2$Si$_1$W$_2$ ingot before and after melt-spinning process are presented in Fig. 1. Base on Fig. 1 (a), the structure of Co$_{78}$Zr$_{17}$B$_2$Si$_1$W$_2$ ingot is combination of pro-peritectic and Zr$_2$Co$_{11}$ phases. The formation of Zr$_2$Co$_{11}$ phase during solidification performs by a peritectic reaction between the primary Co$_{23}$Zr$_6$ and remain liquid phases. The peritectic transformation is a time consuming process and only completes in equilibrium conditions. During conventional solidification, this transformation does not complete and large volume fraction of un-reacted pro-peritectic phase which is composed of Co$_{23}$Zr$_6$ and fcc-Co phases [9, 10] remains in microstructure. In this regard, the FESEM micrographs of Co$_{78}$Zr$_{17}$B$_2$Si$_1$W$_2$ ingot are shown in Fig. 2. As can be seen, there are signs of the pro-peritectic phase in this figure (with a volume fraction of about 35%), which indicates that the peritectic reaction does not complete in this case during conventional casting.

Fig. 1. The XRD patterns of Co$_{78}$Zr$_{17}$B$_2$Si$_1$W$_2$ ingot and melt spun ribbons.

The XRD pattern of melt-spun Co$_{78}$Zr$_{17}$B$_2$Si$_1$W$_2$ sample is presented in Fig. 1 (b). As seen, the number of peaks appearing in these X-ray diffraction patterns is limited and it is very difficult to determine the constituent phases in the prepared ribbons. Various authors have also observed problems, such as overlapping the diffraction peaks, in the X-ray diffraction study of Zr-Co alloying system [6, 7-11]. However, metastable ZrCo$_5$ intermetallic phase is the only hard magnetic phase in the Co-Zr system, and proving the formation of this phase is possible by considering the final hard magnetic properties. Based on the magnetic properties of the studied sample, the single peak in the XRD pattern presented in Fig. 1(b) can be related to metastable ZrCo$_5$ intermetallic phase. The crystallite size of formed ZrCo$_5$ phase was estimated according to Scherrer equation of about 15 nm.

The formation of this non-equilibrium phase and prevention from formation of pro-peritectic and stable phases during melt spinning process can be related to the non-equilibrium conditions which govern in this process. The formation of pro-peritectic phases and transformation of that to Zr$_2$Co$_{11}$ phase is a diffusional process and need more time to complete. Due to the high solidification rate of melt spinning, diffusional processes tends to inhibit and thus the remaining liquid phase experiences a large undercooling before the solidification. In fact, direct transformation of liquid phase to non-equilibrium ZrCo$_5$ during solidification only need to diffusion in short distance and the formation of these phases is kinetically preferred.

2

(a) (b)

Fig. 2. The SEM micrographs of $Co_{78}Zr_{17}B_2Si_1W_2$ ingot in two magnifications.

The hysteresis loops of the $Co_{78}Zr_{17}B_2Si_1W_2$ ingot before and after melt-spinning process are presented in Fig. 3. As seen, the rapid solidification process has significant effect on magnetic properties of prepared samples. The saturation of magnetization and coercivity of $Co_{78}Zr_{17}B_2Si_1W_2$ ingot before melt-spinning process is estimated about 38.4 emu/g and 0.15 kOe, respectively. The low coercively value of this sample can be related to the presence of pro-peritectic and Zr_2Co_{11} phases in the microstructure. However, the melt-spun sample shows so high coercivity value of about 2.7 kOe. In fact, hard magnetic behavior of melt-spun ribbons can be attributed to the precipitation of Co_5Zr hard magnetic phase with high magneto-crystalline anisotropy during melt spinning process. In this regard, Chen et al. [12] reported that the structure obtained in Co-Zr-B system during rapid solidification processes consists of a combination of hard magnetic Co_5Zr and soft magnetic amorphous phases. It has been shown that the strong exchange coupling between hard and soft magnetic phases has been effective in establishing final magnetic behavior.

This means that the dramatic increase in coercivity could be due to the nucleation mechanism of inverse domains. Moreover, the saturation of magnetization value of melt spun ribbons is lower than $Co_{78}Zr_{17}B_2Si_1W_2$ ingot. It is

well known that, the saturation of magnetization depend on the number of aligned spins per unite value. Since, the volume percentage of Co-rich phase reduced during melt spinning process, the saturation of magnetization of as-spun ribbons is lower than ingot.
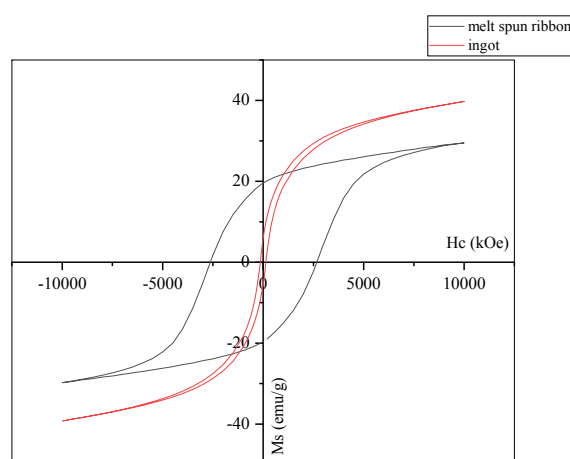
Fig. 3. The room temperature hysteresis loops of $Co_{78}Zr_{17}B_2Si_1W_2$ ingot and melt spun ribbon.

The DSC heating trace of as-spun $Co_{78}Zr_{17}B_2Si_1W_2$ sample is presented in Fig. 4. As seen, there is not any special sharp peak in this DSC curve. To investigation of the structural changes which occur in nanocrystalline $Co_{78}Zr_{17}B_2Si_1W_2$ alloy during annealing, the sample was annealed at 400, 500, 600 and 700ºC for 1 h and the annealed samples were examined

Mohamad Molaahmadi et al.

using XRD and SEM techniques. Based on presented XRD patterns in Fig. 5, during annealing process up to 400ºC, the non-equilibrium $ZrCo_5$ phase progressively transforms to Zr_2Co_{11} phase. This appears to be a structural ordering process which the release/absorption heat during this process is not detectable by DSC analysis. The crystalline sizes of the Zr_2Co_{11} phase in annealed samples were estimated using Scherrer equation.
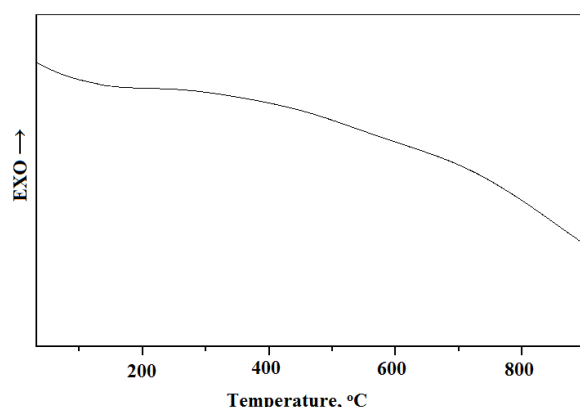
Fig. 4. The DSC heating trace of $Co_{78}Zr_{17}B_2Si_1W_2$ melt-spun ribbons at heating rate of 20ºC/min.

The results showed that, by increasing the annealing temperature, the crystallite size of Zr_2Co_{11} phase increases progressively, and riches to the value of about 800 nm in annealed sample at 700ºC. This result is in agreement with the SEM micrographs of annealed samples which are presented in Fig. 6.

Fig. 5. The XRD patterns for melt-spun ribbons of $Co_{78}Zr_{17}B_2Si_1W_2$ alloys annealed at 400, 500, 600 and 700ºC.

It has been found that annealing of melt spun

materials leads to changes in crystallite size and kind of phases, which have significant effects on magnetic properties. The hysteresis loops of annealed ribbons at different temperature are shown in Fig. 7 and the results are presented in Table 1. Based on this table, several points can be concluded as:

- These hysteresis loops display almost suitable squareness ratio. In fact, high magneto-crystalline anisotropy of $ZrCo_5$ has an impact on the magnetization reversal mechanism named by Stoner-Wohlfarth or domain wall movement and high square ratio in hysteresis loops. However, the kink in the hysteresis loops can be related to the formation of $Co_{11}Zr_2$ phase in annealed samples [10].

- With increasing the annealing temperature, the coercivity of melt-spun ribbons first increases from 2.7 kOe to a maximum value of 3.2 kOe in samples annealed at 400°C and then gradually decreases to about 0.6 kOe in annealed sample at 700°C. The high coercivity of annealed sample at 400°C may be attributed to the fine grain microstructure leading to a single-domain particle-type behavior [13, 14]. Single domain size can be calculated as fallow:

- $D_{crt.} = \frac{9\sigma_W}{2\pi Ms^2}$ (1)

- $\sigma_W = \sqrt{\frac{2K_BT_CK_1}{a}}$ (2)

- Where Ms, T_C, K_B, K_1 are saturation of magnetization, Cure temperature, Boltzmann and anduniaxial anisotropy constant, respectively. By placing of the values of T_C= 723 K, K_B= 1.38×10^{-23} J/K, K_1= 1.1 J/m^3 and M_s= 417.1 emu/cm^3 in this equation, the $D_{crt.}$ value of $ZrCo_5$ phase is estimated about 24 nm. Our calculation shows that, the average crystallite size of $ZrCo_5$ phase in annealed sample at 400ºC (30 nm) is near to $D_{crt.}$ of this phase. In this case, intergrain exchange coupling action strengthens and the effective anisotropy weakens.

- At annealing temperature higher than 400ºC, the $ZrCo_5$ hard magnetic phase transformed to $Co_{11}Zr_2$ phase with soft magnetic characteristics. In fact, increasing of non-equilibrium $ZrCo_5$ crystallite size and decreasing of the percentage of this phase are two main reason of decreasing in Hc value during annealing process.

(a)

(b)

(c)

Fig. 6. The scanning electron microscope images of $Co_{78}Zr_{17}B_2Si_1W_2$ melt-spun ribbons after annealing process at a) 400, b) 550, c) 700ºC.
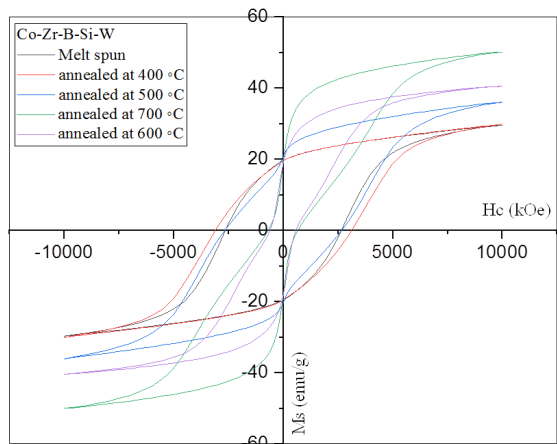
Fig. 7. The room temperature hysteresis loops of $Co_{78}Zr_{17}B_2Si_1W_2$ melt spun ribbons annealed at 400, 500, 600 and 700ºC.

Table 1. The saturation magnetization and the coercivity value of $Co_{78}Zr_{17}B_2Si_1W_2$ melt spun ribbons annealed at different temperatures.

Annealing Temperature (ºC)	Hc (kOe)	Ms (emu/g)
400	3.2	29.5
500	2.7	35.9
600	0.7	40.4
700	0.6	50.3

4. CONCLUSIONS

The structural and magnetic characterization of the nano-crystalline $Co_{78}Zr_{17}B_2Si_1W_2$ alloy with different structure and crystallite size was the major goal of this study. According to achieved results, several conclusions were drawn:

1. Using the melt spinning process at a rotation speed of 40 m/s, single phase Co_5Zr with hard magnetic property was fabricated.
2. The melt spun samples exhibited hard magnetic properties with the coercivity and saturation magnetization values in the range of 2.7 kOe and 29.5 emu/g, respectively.
3. The highest value of coercivity in $Co_{78}Zr_{17}B_2Si_1W_2$ alloy during melt spinning and annealing processes was around 3.2 kOe.
4. The formed Co_5Zr phase was not stable and transformed into the $Co_{11}Zr_2$ phase during annealing. This transformation had detrimental effects on the hard magnetic properties of prepared samples.

REFERENCES

[1]. Balasubramanian, B., Das, B., Skomski, R., Zhang, W.Y., Sellmyer, D.J., "Novel nanostructured rare-earth-free magnetic materials with high energy products". Advanced Materials, 2013, 25, 6090-6093.

[2]. Thanh P.T., Van Duong N., Lam N.M., Hung L.T., Hau K.X., Ngoc N.H., Yen N.H., Dan N.H., "Investigation of structure and magnetic properties of melt-spun Co-Zr-(B, Al) ribbons". Journal of Superconductivity and Novel Magnetism, 2022, 35, 1397-1403.

[3]. Gao, C., Wan, H., Hadjipanayis, G.C., "High coercivity in non rare-earth containing alloys". Journal of Applied Physics, 1990, 67, 4960-4962.

[4]. Lucis, M.J., "Microstructure and phase analysis in Mn-Al and Zr-Co permanent magnets". University of Nebraska-Lincoln, 2015.

[5]. Saito, T., "The origin of the coercivity in Co-Zr system alloys". IEEE Transactions on Magnetics, 2003, 39, 2890-2892.

[6]. Saito, T., Itakura, M., "Microstructures of Co-Zr-B alloys produced by melt-spinning technique". Journal of Alloys and Compounds, 2013, 572, 124-128.

[7]. Palit, M., Chelvane, J.A., Basumatary, H., Babu, D.A., Kamat, S.V., "Microstructure and magnetic properties in as-cast and melt spun Co-Zr alloys". Journal of Alloys and Compounds, 2015, 644, 7-12.

[8]. Zhang, W.Y., Li, X.Z., Valloppilly, S., Skomski, R., Shield, J.E., Sellmyer, D.J., "Magnetism of rapidly quenched rhombohedral Zr2Co11-based nanocomposites". Journal of Applied Physics D, 2013, 46, 135004.

[9]. Shifeng Xu, D.X., Hou, Z., Zhang, J., Su, F., Sun, L., Wang, W., "The Structure and Magnetic Properties of $Co_{77}Zr_{18}W_5$ Melt-Spun Ribbons". Journal of Condensed Matter Physics, 2012, 2, 197-201.

[10]. Zhang, W., Valloppilly, S.R., Li, X., Skomski, R., Shield, J.E., Sellmyer, D.J., "Coercivity enhancement in $Co_{11}Zr_2$-based nanocrystalline materials due to Mo addition". IEEE Transactions on Magnetics, 2012, 48, 3603-3605.

[11]. Saito, T., "Microstructures and magnetic properties of Co-Zr system alloys". Materials Transactions, 2003, 44, 1713-1716.

[12]. Chen, L.Y., Chang, H.W., Chiu, C.H., Chang, C.W., Changa W.C., "Magnetic properties, phase evolution and coercivity mechanism of $Co_xZr_{98-x}B_2$ (x= 74-86) nanocomposites". Journal of Applied Physics, 2005, 97, 10F307.

[13]. Matyja, J.J.H., "Studies on crystallization and domain structure of a romagnetic amorphous alloy Co-Zr". Journal of Material Science, 1980, 15, 2317-2321.

[14]. Balamurugan, B., Das, B., Zhang, W.Y., Skomski, R., Sellmyer, D.J., "Hf-co and Zr-Co alloys for rare-earth-free permanent magnets". Journal of Physics: Condensed Matter, 2014, 26, 062204.